Memory properties of spatially-extended disordered materials

Enrique García Ortiz
Facultat de Física, Universitat de Barcelona, Martí i Franquès 1, 08028 Barcelona, Spain.

Advisor: Jordi Ortín Rull

Abstract: Memory is a fascinating phenomenon that has many interesting applications. This work focuses on Return-Point Memory (RPM), which is a particular type of memory present on ferromagnetic, spatially-extended disordered systems that manifests through quasistatic hysteresis. By modelling these materials using the fluctuationless Random Field Ising Model (T=0 RFIM) and computing the magnetization trajectories via a cellular automaton, we observe RPM, thus proving the validity of the model for this purpose, and analyze it qualitatively both at macroscopic and microscopic scales. We also perform a study on energy dissipation in this model and its relation with hysteresis and Barkhausen magnetization jumps.

I. INTRODUCTION

Memory is a phenomenon that has been observed in many different systems; from living biological systems to glassy solids and complex fluids. It is often defined as the capacity that systems have to store information and their ability also to access it and wipe it out [1]. This paper will focus on a type of memory called Return-Point Memory (RPM), which plays a key role in hysteresis.

Hysteresis (from the greek, lag or delay) shows up when the system does not react promptly if we change a control parameter, so a certain delay in the response of the system (the order parameter) appears. On general grounds, there are two types of hysteresis: rate-dependent and rate-independent. When the hysteresis is rate-dependent, the time scale of forcing is comparable to the time scale of relaxation of the system, whereas when it is rate-independent the relaxation happens to be much faster than the driving. The latter is also known as quasistatic hysteresis or intrinsic hysteresis, since the driving can be infinitely slow and the system will still display hysteresis (unlike the former where the phenomenon dissapears if the driving is too slow). In this work we will focus on quasistatic hysteresis as we want to study intrinsic memory properties of the materials.

The control and order parameters are typically the applied field (H) and the magnetization of the system (M), respectively, as many systems that exhibit hysteresis are magnetic (and we assume that their magnetism is strongly anisotropic, with M being the magnetization along the easy axis); but this effect can be generated from many different conjugate parameter pairs, as hysteresis is common in other out-of-equilibrium systems, such as ferroelectricity, ferroelasticity, hydrology, etc. [2]. For example, the hysteresis shown in Ref. [3] for ferroelastic materials originates from the stress-strain pair. The delay that characterizes hysteresis greatly influences the $H(M)$ curve and makes it irreversible: the path that the system follows while H is increasing (increasing magnetization) will not be the same as the path it follows when H is decreasing (demagnetization). Thus, if we start from a sufficiently negative value of H such that the magnetization is saturated to its most negative possible value, increasing H monotonously gives rise to the outer curve of increasing magnetization shown in Fig. 1, curve (a). Equivalently, from the positive value of saturation magnetization, a decreasing excursion of H produces the descending curve (a) of Fig. 1. The result is the widest possible hysteresis cycle of the system. However, if we had interrupted the descending curve (a) at a given value of H and reversed its direction back to the saturation magnetisation again, we would generate what is called a First-Order Reversal Curve (FORC) that explores the inner area within the cycle. An equivalent FORC could also be entraced from the ascending curve (a) down to the negative saturation magnetization value. During the inner exploration of a FORC the RPM property shows up: the point in which the direction inversion was done gets "memorized" in the system. A second change of direction while the system is still on a FORC will always produce another curve (Second-Order Reversal Curve or SORC) that will end on the return point, forming an inner cycle (Fig. 1, curve (b)). The properties of the inner cycle depend on the position of the return point in the main cycle so that the system keeps memory of this re-

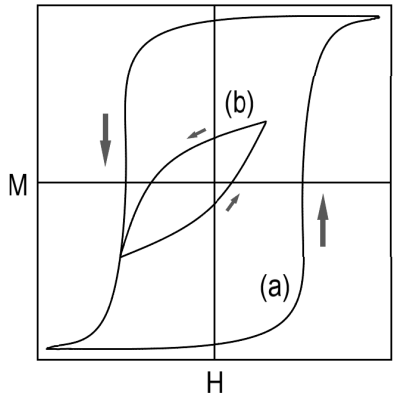

FIG. 1: Schematic representation of the hysteresis cycle of a ferromagnetic system. The direction of the variation of H is indicated with some arrows, and the different hysteretic curves are labeled with (a) and (b).

turn point. However, once the system reaches the return point again, this memory gets erased and the system follows normally the outer cycle until saturation. This will be referred to as "wiping out". Moreover, it is also possible to recur this procedure while the system is still on an inner cycle. In this case, a cycle within the cycle will be formed and a second return point will be stored. Further recursions lead to more cycles within cycles and more return points being recorded, but the system will record them with a certain hierarchy: the system cannot access the data of the first return point without accessing and erasing the information of all the return points that were recorded afterwards.

Throughout the last century various models of quasistatic hysteresis were developed. An important one is the Preisach model, which is more of a "black-box" type [4]. In the present work we will focus on the Random Field Ising Model at zero temperature ($T = 0$ RFIM), as it gives a microscopic view of the phenomena that helps explaining the physical, macroscopic hysteresis that is observed [5]. The T=0 RFIM is a minor modification of the well-known Ising model that essentially introduces disorder to the system. This disorder is a crucial ingredient of the model. It gives rise to magnetization avalanches (Barkhausen jumps) extending over a wide range of applied magnetic fields. Moreover, as Sethna et al demonstrated in Ref. [5], it mediates a first-order phase transition between a non-hysteretic phase in which spins flip in an uncorrelated manner and a hysteretic phase in which avalanches of spin flips are triggered by the disorder. This amazing discovery invigorated a new wave of studies to generalize this disorder-controlled transition to more systems and models than the T=0 RFIM originally proposed by Sethna [6].

The objectives of this study are to write the code of a T=0 RFIM as a cellular automaton, to prove that it presents hysteresis even if the driving is quasistatic, to study memory properties using the inner cycles and, finally, to analyze the energy dissipation in the model and how it correlates with the discrete magnetization jumps.

It has been demonstrated that other types of cellular automata such as the deterministic sandpile models also present hysteresis and RPM [7]. For this reason we have considered that understanding the fluctuationless RFIM as a cellular automaton will be beneficial towards achieving the first of the objectives described before. The cycles displayed in this work correspond to 2D systems composed of $L \times L$ spins, with $L = 64$ and periodic boundary conditions. We will first establish in Sec. II the rules of the cellular automaton that represents the T=0 RFIM and clarify how we simulate the hysteresis cycles. Next, in Sec. III we will focus on RPM (specially on the demonstration presented in Ref. [5]) and we will prove that our cycles exhibit this property. Lastly, in Sec. IV we will change topics and put the spotlight on the energy dissipation concomitant to hysteresis and its correlation with the magnetization jumps.

II. THE T=0 RFIM AS A CELLULAR AUTOMATON

The fluctuationless RFIM can be characterized using the following hamiltonian, based on the typical Ising model (in this study we will fix $J \equiv +1$ for ferromagnetic behavior):

$$\mathcal{H} = -\sum_{\langle i,j \rangle} s_i s_j - H \sum_i s_i - \sum_i h_i s_i, \qquad (1)$$

where the first and second terms are the contribution to $\mathcal{H}$ of first-neighbors interaction and the applied magnetic field, both present in the Ising model. The third term gives rise to the model's name, since it represents the contribution of the interaction with the random fields, h_i. These are local magnetic fields that are quenched on each lattice site, and may represent magnetic impurities of the material. An alternative writing of Eq. (1) is:

$$\mathcal{H} = -\sum_i F_i s_i; \qquad F_i \equiv \sum_{\langle j|i \rangle} s_j + H + h_i, \qquad (2)$$

where F_i refers to the total magnetic field that the spin at position i experiences. To simulate this model as a cellular automaton, initially, we establish a 2D $L \times L$ lattice and generate $\mathcal{N} \equiv L^2$ random field values, following a Gaussian distribution centered at $\mu = 0$ and distributed through the lattice with a certain standard deviation σ. The spin on each site has two well-defined states: "up" ($s_i = +1$) and "down"($s_i = -1$). Since the system is simulated at $T = 0$, it does not experience thermal fluctuations. A spin will flip only when its local field changes sign, so that the hamiltonian in Eq. (2) is minimized. Therefore, the spins will evolve between states following the rule:

$$F_i s_i \leq 0 \quad \Rightarrow \quad s_i \to -s_i. \qquad (3)$$

In each iteration step, first we fix a value of the external field H. Then, we go across the $\mathcal{N}$ different sites checking Eq. (3). If it becomes true, the position i is noted down. Only when all $\mathcal{N}$ sites have been checked will the entirety of noted values be flipped *synchronously*. After these first flips, the F_i of sites that were first-neighbors of one of the flipped spins may have changed and now they may satisfy the condition of Eq. (3). Next, the sweeping across the $\mathcal{N}$ different sites and the synchronous flipping must be iterated until a sweeping results on none of the sites satisfying the condition. This whole updating is defined as an avalanche, as a spin flip may have caused a flip of some of its first neighbors, and so on, in a collective process. Once the avalanche stops, this step is completed, and we must proceed to the next value of H. When simulating, we cleverly decide the next relevant value of H by keeping track of which random fields are associated with the spins "up" or "down" and calculating the next value that would cause, at least, one flip. To change the direction of H at the hysteresis cycle we simply change

the list of "down" spins by the list of "up" spins or vice versa. Each simulation starts with all spins "down", then we start magnetizing (flipping spins to "up") until all spins are "up". We complete the cycle demagnetizing (flipping spins to "down"), though during this process we change from demagnetizing to magnetizing and so on arbitrarily in order to achieve FORCs and SORCs and manifest RPM. This will be explored further on the next section.

The cycles that result from this kind of simulations exhibit what is known as Barkhausen effect: the field variations correspond to the horizontal lines, while the avalanches translate into the vertical jumps in Fig. 2.

III. DISPLAY OF MEMORY PROPERTIES

In this section we will show that our simulations display the RPM described in the Introduction.

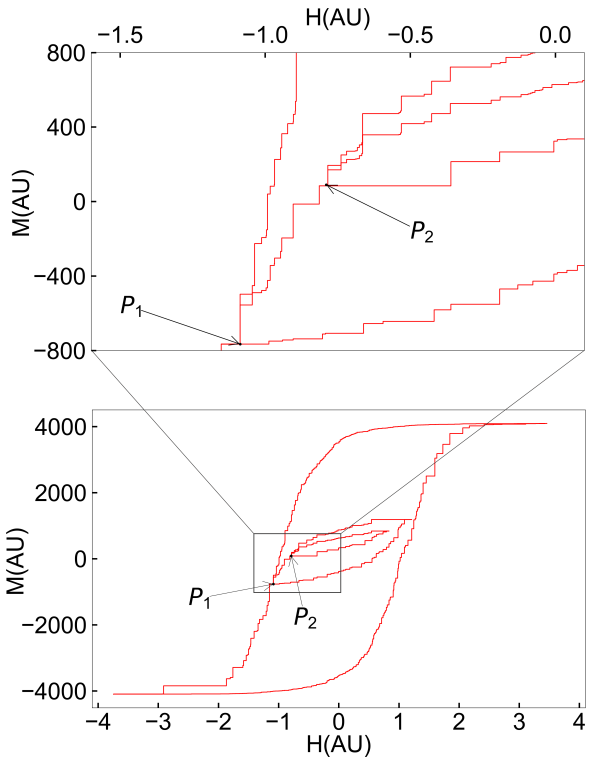

FIG. 2: Hysteresis cycle $M(H)$ generated via simulation fixing $\sigma = 2.2$, with an additional inner cycle inside the first one to prove the hierarchical nature of RPM. The inset zooms in on the trajectories near the return points.

Figure 2 confirms that our cellular automaton is capable of reproducing the RPM property that the T=0 RFIM presents. Analyzing the figure with more detail, we can appreciate that a FORC is performed at P_1 while the system is demagnetizing. Before letting the system return to P_1 with a SORC, we change the direction of H once again at P_2. The innermost cycle starts and ends exactly at P_2, and the middle cycle finally arrives exactly at P_1. This figure also illustrates very well both the "wiping out" property (the system erases both P_1 and P_2 once it has accessed each point) and the hierarchical nature of the stored points (P_2 must be accessed and erased in order to reach P_1).

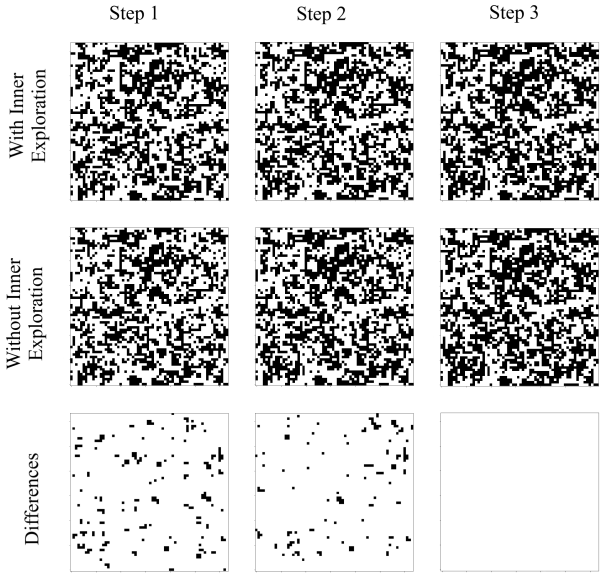

FIG. 3: Comparative figure of different microstates of a disordered, ferromagnetic system. This particular simulation has been done with a particularly high σ ($\sigma = 5.4$). The first two rows show the "up" and "down" sites painted as white and black, respectively. The third shows in black the sites that are not in the same state in both previous rows. Step 3 corresponds to the return point. Taking it as a reference, the other steps are 10 steps away from each other and correspond to the demagnetization trajectories along the SORC (first row) and along the outer path (second row).

We can extend this study to the microscopic scale. Figure 2 proved that at macroscopic scale the system exhibits memory (it "remembers", at least, the point (H, M) at which the FORC starts), but Fig. 3 takes it a step further. Not only the values of H and M are stored, but the system returns to the *same exact spin configuration* $\{s_i\}$ after traversing an inner cycle.

This result concurs with Ref. [5]: given a system that evolves following an applied field $H(t)$ so that $H(0) \leq H(t) \leq H(T)$ for a time $0 \leq t \leq T$, the final configuration of the system will only depend on $H(T)$ and will be completely independent of the rest of parameters, such as the particular path done by $H(t)$. This property is based on three key points:

- Since the model is fluctuationless (T=0), the system evolution is deterministic: given a system that starts at $\{s_i\}_A$ and H_A, and ends at H_B, all monotonic paths that the applied field can follow to go to H_B will make the system evolve to the same microstate $\{s_i\}_B$.

- There is a partial ordering of the possible microstates. Given two states $\{s_i\}$ and $\{r_i\}$, we consider $\{s_i\} \leq \{r_i\}$ if and only if $s_i \leq r_i \ \forall i = 1, 2, \ldots, \mathcal{N}$.
- The system follows what is known as *Middleton's no-passing rule*: given two states $\{s_i\}$ and $\{r_i\}$ that satisfy $\{s_i\}(0) \leq \{r_i\}(0)$ and evolve under respective fields $H_s(t) \leq H_r(t)$, then it is true that $\{s_i\}(t) \leq \{r_i\}(t) \ \forall t$. This is equivalent to affirm that *the partial ordering is preserved by the deterministic dynamics*. See Refs. [5, 7].

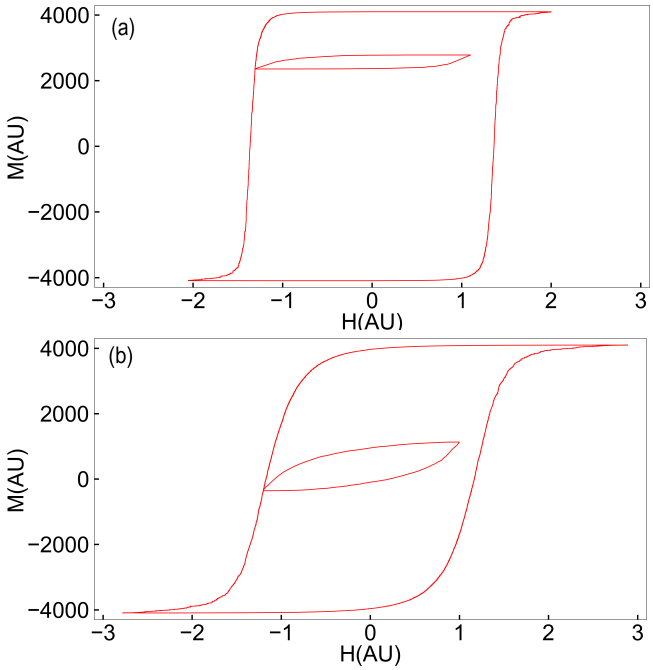

FIG. 4: Hysteresis cycles $M(H)$, averaged using 100 realizations of the simulation program each. The difference between the two subfigures is the variance σ taken to generate the random field values ($\sigma = 1.1$ and $\sigma = 1.7$ for (a) and (b), respectively).

Lastly, it is worth noting that averaging multiple different simulations done with the same parameters results on cycles that do not present the Barkhausen effect but still exhibit memory (macroscopically, at least). Figure 4 evidences this last statement and also proves that the system displays memory regardless of the standard deviation σ chosen to generate the random field values. Nevertheless, it has been demonstrated that the variance σ of the random field distribution greatly affects the shapes of these cycles, as Fig. 4 exposes: at low values of σ the cycles tend to have various-sized avalanches (a few of them are large while the rest are rather small), whereas high values of σ generate cycles with a larger number of avalanches overall but with lower, more consistent size. Several researches had the objective of finding the value of σ that acts as a boundary between the two behaviors, σ_c [5, 8]. However, σ_c depends on the size and the dimension of the system, so the values given by these authors are not applicable to our simulations. The value of σ_c specific to our system must be found between the values $\sigma = 1.1$ and $\sigma = 1.7$ used for Fig. 4.

IV. ENERGY DISSIPATION

In the previous section we already distinguished between the macroscopic and the microscopic scales. The following study on energy dissipation helps us delve deeper into the relation between these scales, since the hysteresis cycles that we can observe at macroscopic scale result from the energy dissipated in the spin flips. This energy can reach significant values when the flipping is done collectively in the form of avalanches. The main purpose of this section is to investigate the relationship between magnetization jumps and the corresponding energy losses.

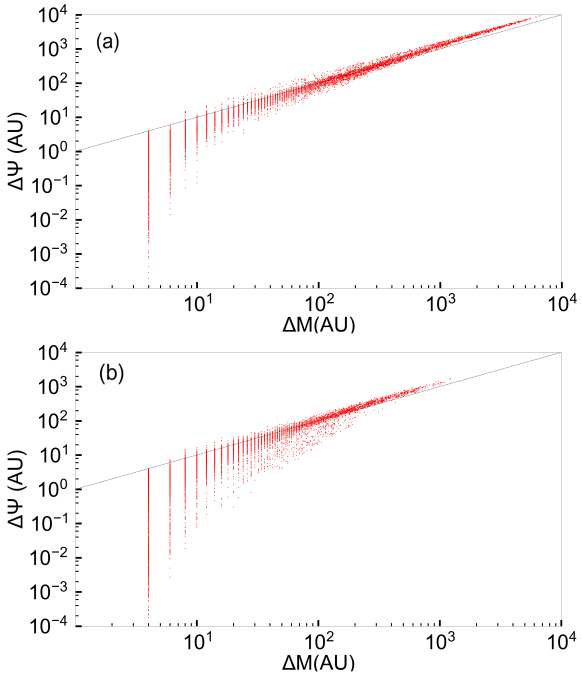

FIG. 5: Double-logarithmic representation of the amount of energy dissipated in an avalanche versus the avalanche size, represented by the change of magnetization in the avalanche. Again, two behaviors have been studied taking the same values of σ as Fig. 4. The dashed line that appears in both figures corresponds to the relation $y \propto x$ that a linear function would display.

To analyze energy dissipation, we may symbolically differentiate the hamiltonian:

$$d\mathcal{H} = -\sum_i^n F_i ds_i - \sum_i^n s_i dF_i, \tag{4}$$

where n refers to the number of spins that flip during a particular avalanche. Regarding the second term, it can be simplified to $-\sum_i^n s_i dH \equiv -M dH$, as the random

fields do not change and the first-neighbor interactions are already considered within the synchronous dynamics. Following Ref. [9], $\mathcal{H} = U - HM$, where U is the internal energy of the system, and the energy balance in an avalanche reads $dU = HdM - đ\psi$, where HdM is the energy that the driving field supplies and $đ\psi$ is the dissipated energy. This last contribution is then:

$$đ\psi = HdM - dU = -MdH - d\mathcal{H} = \sum_i^n F_i ds_i. \qquad (5)$$

Next we show that, contrary to what could be naively expected, the energy dissipated in an avalanche and the corresponding change of magnetization are not proportional to each other. We are basically comparing the following differentials:

$$đ\psi = \sum_i^n F_i ds_i; \qquad dM = \sum_i^n ds_i, \qquad (6)$$

which show that the ds_i are weighted by the local fields F_i in the expression for $đ\psi$. Figure 5 compares these variables using logarithmic scales. If they were linearly related the points would adjust to the presented slope, but they clearly deviate from it: at low avalanche sizes there are many different amounts of energy dissipated (to the point that they are orders of magnitude apart) whereas at high avalanche sizes the dissipated energy tends to be higher than what a linear relation would predict. The results agree with the results of Ref. [9]: the energy dissipation is not proportional to the size of the corresponding magnetization jump.

V. CONCLUSIONS

By writing a program that treats the fluctuationless RFIM as a cellular automaton, we have been able to simulate the typical quasistatic hysteretic behavior of ferromagnetic, extended disordered materials. We have studied the memory properties that the generated cycles exhibited and found that they satisfactorily display RPM as it is predicted for both the T=0 RFIM [5] and other types of deterministic cellular automata [7]. Some particularities of RPM such as the "wiping out" property and the return-point hierarchy have also been successfully verified. This property has been displayed at both macroscopic and microscopic scales, as the system returns to the same state that it departed from when the FORC initiated (same values of H and M *and* same spin configuration $\{s_i\}$).

Next, we performed averages over 100 realizations of the random fields with the same parameters and proved that RPM is not lost by conducting these averages. We also noted the two possible behaviors of the average cycles based on the standard deviation σ used to obtain the random field values from a Gaussian distribution. Although the exact value of the boundary σ_c has not been determined, it has been enclosed by the values used for Fig. 4.

Finally, we also analyzed the dependence that the energy dissipated in each avalanche could have with its size. After a double-logarithmic representation (Fig. 5), we have concluded that there is no clear correlation between the two of them, in concordance with Ref. [9]. This representation also served to classify the type of avalanches that are present in each behavior and further characterize them.

Acknowledgments

First of all, I would like to express my deepest gratitude to my advisor, Jordi Ortín. I really appreciate his dedication to advising and guiding me through the realization of this work, and I am really grateful for all the things I learned under his tutelage.

I would also like to thank my family and friends for their constant support, not only during the writing of this paper but for all these years that I have been studying Physics.

[1] N. C. Keim, J. D. Paulsen, Z. Zeravcic, S. Sastry and S. R. Nagel, *Memory formation in matter*. Rev. Mod. Phys. **91**, 035002 (2019).

[2] *The Science of Hysteresis* (three-volume Book Series), G. Bertotti and I.D. Mayergoyz Eds., Academic Press, Oxford (2006).

[3] J. Ortín, *Preisach modeling of hysteresis for a pseudoelastic Cu-Zn-Al single crystal*. J. Appl. Phys. **71**, 1454 (1991).

[4] I. D. Mayergoyz, *Mathematical Models of Hysteresis*. Springer-Verlag, New York (1991).

[5] J. P. Sethna, K. Dahmen, S. Kartha, J. A. Krumhansl, B. W. Roberts and J. D. Shore, *Hysteresis and hierarchies: Dynamics of Disorder-Driven First-Order Phase Transformations*. Phys. Rev. Lett. **70**, 3347 (1993).

[6] E. Vives, J. Goicoechea, J. Ortín and A. Planes, *Universality in models for disorder-induced phase transitions*. Phys. Rev. E **52** R5 (1995).

[7] J. Goicoechea and J. Ortín, *Hysteresis and Return-Point Memory in Deterministic Cellular Automata*. Phys. Rev. Lett. **72**, 2203 (1994).

[8] F. J. Pérez-Reche and E. Vives, *Finite-size scaling analysis of the avalanches in the three-dimensional Gaussian random-field Ising model with metastable dynamics*. Phys. Rev. B **67**, 134421 (2003).

[9] J. Goicoechea and J. Ortín, *Dissipation in quasistatically driven disordered systems*. Phys. Rev. B **58**, 5628 (1998).